Thermoelectric Materials

International Edition: DOI: 10.1002/anie.201508492
German Edition: DOI: 10.1002/ange.201508492

Tailoring of Electronic Structure and Thermoelectric Properties of a Topological Crystalline Insulator by Chemical Doping

*Subhajit Roychowdhury, U. Sandhya Shenoy, Umesh V. Waghmare, and Kanishka Biswas**

Abstract: *Topological crystalline insulators (TCIs) are a new quantum state of matter in which linearly dispersed metallic surface states are protected by crystal mirror symmetry. Owing to its vanishingly small bulk band gap, a TCI like $Pb_{0.6}Sn_{0.4}Te$ has poor thermoelectric properties. Breaking of crystal symmetry can widen the band gap of TCI. While breaking of mirror symmetry in a TCI has been mostly explored by various physical perturbation techniques, chemical doping, which may also alter the electronic structure of TCI by perturbing the local mirror symmetry, has not yet been explored. Herein, we demonstrate that Na doping in $Pb_{0.6}Sn_{0.4}Te$ locally breaks the crystal symmetry and opens up a bulk electronic band gap, which is confirmed by direct electronic absorption spectroscopy and electronic structure calculations. Na doping in $Pb_{0.6}Sn_{0.4}Te$ increases p-type carrier concentration and suppresses the bipolar conduction (by widening the band gap), which collectively gives rise to a promising zT of 1 at 856 K for $Pb_{0.58}Sn_{0.40}Na_{0.02}Te$. Breaking of crystal symmetry by chemical doping widens the bulk band gap in TCI, which uncovers a route to improve TCI for thermoelectric applications.*

Topological insulators (TIs) have drawn an immense interest in chemistry and material science recently, owing to their unique conductive properties.[1] TIs are a new quantum state of matter with a bulk band gap typically generated by a strong spin orbit coupling and topologically protected linearly dispersed metallic surface states.[1] TIs have different electronic structures compared to conventional semiconductors and insulators with special characteristic topologically protected metallic surface states.[2] TIs possess an odd number of band inversions between valence and conduction band owing to strong spin orbit coupling.[3] Metallic surface states of TIs are protected by time-reversal symmetry, thus surface states in TIs are robust against almost any type of chemical surface modification.[3] Many TIs are known to be excellent thermoelectric (TE) materials because of the requirement of similar features in the electronic band structure.[4] The primary criteria for good TE and TI materials are relatively similar as both require heavy elements and narrow band gap semiconducting electronic structure.[4]

TCIs are a new class of topological materials[5] that are fundamentally different from conventional TIs in terms of their surface state protection mechanism. TI surface states are protected by time-reversal symmetry, while TCI surface states are protected by crystal mirror symmetry.[5] Thus, breaking of crystal symmetry can alter the electronic structure of TCI. Recently, crystal symmetry in TCI was broken by various external physical perturbations, such as by applying electric fields, ferroelectric structural distortion, mechanical strain, and thickness engineering.[5,6]

Recently, solid solution composition, $Pb_{0.6}Sn_{0.4}Te$,[7] derived from the well-known thermoelectric materials, PbTe ($E_g \approx 0.29$ eV)[4] and SnTe ($E_g \approx 0.18$ eV, inverted gap),[8] has been discovered to be a TCI by angle-resolved photoemission spectroscopy (ARPES).[9] High-resolution scanning tunnelling microscopy/spectroscopy measurements revealed the crystal symmetry-breaking and distortion of the surface of TCI, which resulted in opening of band gap and massive Dirac fermion formation.[5e,i] Furthermore, applying an electric field perpendicular to the thin films of SnTe and $Pb_{1-x}Sn_xSe(Te)$ grown along (001) direction breaks the mirror symmetry, resulting in the opening of a band gap from the edge states.[5d] Although chemical doping should alter the electronic structure of TCI by perturbing the local mirror symmetry in the crystal structure, breaking of mirror symmetry in TCI has been mostly explored by physical perturbation techniques so far. Efforts to make chemical modification of a TCI have not yet been reported.

Herein, we report the effect of sodium (Na) doping on the electronic structure and thermoelectric properties of crystalline ingots of the TCI, $Pb_{0.6}Sn_{0.4}Te$. Na doping in $Pb_{0.6}Sn_{0.4}Te$ breaks the local mirror symmetry, resulting in the opening of a band gap, which is observed by both direct band gap measurement through electronic absorption spectroscopy and first-principles density functional electronic structure calculations. Na doping increases the p-type carrier concentration in $Pb_{0.6}Sn_{0.4}Te$, which pushes the Fermi level deeper into the valence band. The increase in the band gap after Na doping suppresses the bipolar conduction in $Pb_{0.6}Sn_{0.4}Te$. This pushes the temperature-dependent Seebeck maximum to higher temperature and decreases the thermal conductivity further at higher temperature. We have achieved a maximum thermoelectric figure of merit (zT) of ≈ 1 at 856 K for $Pb_{0.58}Sn_{0.40}Na_{0.02}Te$, which is significantly higher compared to undoped TCI, $Pb_{0.6}Sn_{0.4}Te$ ($zT \approx 0.38$ at 475 K).

First, high-quality crystalline ingots of $Pb_{0.6-x}Sn_{0.4}Na_xTe$ ($x = 0$, 0.01, 0.02, 0.03, 0.04) were synthesized by mixing appropriate ratios of high-purity starting materials of Sn, Pb,

[*] S. Roychowdhury, Dr. K. Biswas
New Chemistry Unit, Jawaharlal Nehru Centre for Advanced Scientific Research (JNCASR)
Jakkur P.O., Bangalore (India)
E-mail: kanishka@jncasr.ac.in
Homepage: http://www.jncasr.ac.in/kanishka/
Dr. U. S. Shenoy, Prof. Dr. U. V. Waghmare
Theoretical Science Unit, Jawaharlal Nehru Centre for Advanced Scientific Research (JNCASR)
Jakkur P.O., Bangalore 560 064 (India)

Supporting information for this article is available on the WWW under http://dx.doi.org/10.1002/anie.201508492.

Na, and Te in a quartz tube by vacuum-sealed tube melting reaction. The quartz tubes were sealed under vacuum (10^{-5} torr), slowly heated up to 1323 K, and then slowly cooled down to room temperature (see the Supporting Information).

The powder X-ray diffraction (PXRD) pattern of $Pb_{0.6-x}Sn_{0.4}Na_xTe$ ($x = 0$–0.04) could be indexed based on the cubic PbTe structure (space group, $Fm\bar{3}m$; Figure 1a). No other peak was observed within the detection limit of the PXRD data, which establishes the formation of single-phase materials.

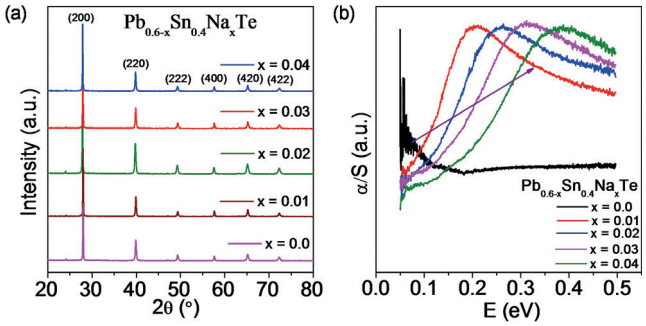

Figure 1. a) Powder X-ray diffraction pattern and b) electronic absorption spectra for $Pb_{0.6-x}Sn_{0.4}Na_xTe$ ($x = 0$–0.04) samples.

Recently, ARPES measurements have confirmed the topological crystalline insulator phase in $Pb_{0.6}Sn_{0.4}Te$ with nearly zero electronic band gap.[9] Previous band inversion models also predicted zero band gaps in $Pb_{0.6}Sn_{0.4}Te$.[10] We have measured the band gap of several samples in the $Pb_{0.6-x}Sn_{0.4}Na_xTe$ ($x = 0$–0.04) composition by infrared (IR) diffuse reflectance spectroscopy (Supporting Information). We were not able to resolve the band gap of $Pb_{0.6}Sn_{0.4}Te$ by IR diffuse reflectance spectroscopy as the band gap energy is nearly 0 eV (Figure 1b). Interestingly, with increasing sodium doping concentration from 1 to 4 mol%, the band gap systematically increases from ≈0.1 eV to ≈0.22 eV, respectively (Figure 1b; Supporting Information, Figure S1). Substitution of Na in place of Pb in $Pb_{0.6}Sn_{0.4}Te$ breaks the local crystal mirror symmetry, which lifts the protection to the metallic surface states, opening up the band gap.

To understand the effects of Na doping on the electronic structure of $Pb_{0.6}Sn_{0.4}Te$ in detail, we determined and compared the electronic structure of $Pb_{0.6}Sn_{0.4}Te$ and Na-doped (6 mol%) $Pb_{0.6}Sn_{0.4}Te$. We consider two symmetry inequivalent structures of $Pb_9Sn_6NaTe_{16}$, by choosing two inequivalent sets of sites for substitution of Na (Figure 2a). In the first one (I), the inversion symmetry is retained, whereas the inversion symmetry is broken in the second configuration (II). From the electronic structure of $Pb_{10}Sn_6Te_{16}$, it is clear that the band gap is nearly zero (Figure 2b), in agreement with the results of band gap measurements using diffuse reflectance IR spectroscopy. It is also evident that the valence band peaks slightly away from the Γ point, giving it a hole-like character, and the conduction band is almost flat, barely touching the Fermi level, giving it an electron-like character with high density of

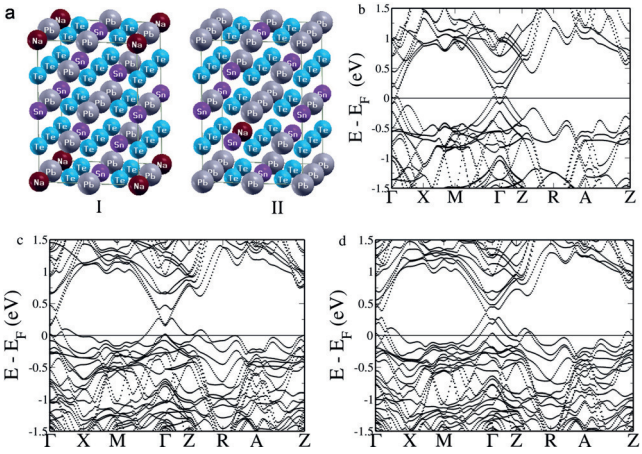

Figure 2. a) Crystal structure of $Pb_9Sn_6NaTe_{16}$ with (I) and without (II) retaining mirror symmetry. b) Electronic structure of undoped $Pb_{10}Sn_6Te_{16}$. c) Electronic structure of $Pb_9Sn_6NaTe_{16}$ with retaining mirror symmetry. d) Electronic structure of $Pb_9Sn_6NaTe_{16}$ without retaining mirror symmetry showing opening up of the band gap. All the energies are shifted with respect to the Fermi energy, which is equal to zero. The VBM and CBM occurring at L point in the rocksalt cell fold on to the Γ point and the heavy hole valence band appearing along Σ folds onto $Z+\delta$ in the case of the present 32 atom $(\sqrt{2}\times\sqrt{2}\times\sqrt{2})$ tetragonal supercell.

states. Upon substitution of Na, the Fermi level shifts to a lower energy such that hole-like orbits centered at many low symmetry k points emerge. The contribution of Na atomic orbitals is seen in the higher energy conduction bands (2 eV above the Fermi level). In the centrosymmetric configuration of Na substitution, we see that the electronic structure near Fermi level is symmetric on the two sides of Γ point (M-Γ and Γ-Z) (Figure 2c) and the system is almost metallic. In contrast, when Na substitution lowers the structural symmetry a band gap opens up (0.037 eV; Figure 2d), which indeed supports the experimental band gap results. The degeneracy of bands above Fermi level is lifted around Γ point. Visualization of wave functions of states at Γ point and slightly above the Fermi level reveals the primary contribution from *p* orbitals of Pb. We find that the lower symmetry of the configuration (II) results in mixing and reshuffling of bands that open up the gap.

The positive sign of the Hall coefficient suggests *p*-type conduction in the $Pb_{0.6-x}Sn_{0.4}Na_xTe$ ($x = 0$–0.04) sample. When the Na doping concentration is increased from 0 to 4 mol%, p-type carrier concentration increases from $\approx 9.44\times10^{18}$ cm^{-3} to 5.69×10^{19} cm^{-3}. Each Na^+ substitutes for Pb^{2+} and, from simple valence counting, contributes one extra p-type carrier, pushing the Fermi level further inside the valence band of $Pb_{0.6}Sn_{0.4}Te$, which is consistent with the theoretical calculation results.

The opening of the electronic band gap and the increase in p-type carrier concentration motivated us to measure the thermoelectric properties in the 300–873 K range. Previously, promising thermoelectric properties were observed in Na-doped PbTe owing to the contribution of a heavy hole valence band of PbTe in thermoelectric transport at higher temperature.[11,12] Electrical conductivity (σ) of $Pb_{0.6-x}Sn_{0.4}Na_xTe$ ($x =$

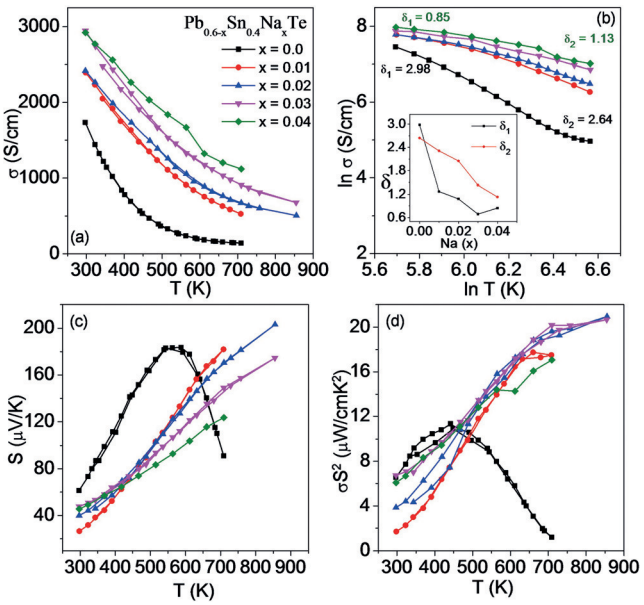

Figure 3. a) Temperature-dependent electrical conductivity (σ) of $Pb_{0.6-x}Sn_{0.4}Na_xTe$ ($x = 0$–0.04) samples. b) ln σ as a function of ln T; inset of (b) shows the Na concentration-dependent δ values. Temperature-dependent (c) Seebeck coefficient (S) and (d) power factor (σS^2) of $Pb_{0.6-x}Sn_{0.4}Na_xTe$ ($x = 0$–0.04) samples.

0–0.04) samples as a function of temperature are shown in Figure 3a. The σ value for all samples decreases with increasing temperature, which is consistent with the behavior of a degenerate semiconductor. Room temperature σ increases significantly from $\approx 1725\ S\,cm^{-1}$ in $Pb_{0.6}Sn_{0.4}Te$ to $\approx 2941\ S\,cm^{-1}$ for 4 mol% Na-doped $Pb_{0.6}Sn_{0.4}Te$, which is mainly attributed to the increase in carrier concentration owing to Na doping. Temperature-dependent σ can be fitted to the equation $\sigma \approx T^{-\delta}$ to extract the scattering mechanism, which was earlier employed in Na-doped PbTe.[12] Two different values of scattering factor δ (δ_1 in low temperature region and δ_2 in the high temperature region) were extracted from the lnσ versus ln$T$ plot for Na-doped $Pb_{0.6}Sn_{0.4}Te$ samples (Figure 3b), which decrease with increasing Na concentration (inset in Figure 3b). Two scattering factors denote the contributions from both light hole (L point) and heavy hole (Σ point) valence bands to the temperature-dependent electronic transport.[13] The smaller δ values in Na-doped samples implies a much weaker temperature-dependence of hole scattering at higher temperature.

The Seebeck coefficient of $Pb_{0.6-x}Sn_{0.4}Na_xTe$ ($x = 0$–0.04) samples as a function of temperature is shown in Figure 3c. With increasing temperature, the Seebeck coefficient of undoped $Pb_{0.6}Sn_{0.4}Te$ initially increases and reaches a maximum at ≈ 550 K, then decreases with further increases in the temperature up to 700 K, which is typical of bipolar conduction in a narrow band gap semiconductor. Na doping in $Pb_{0.6}Sn_{0.4}Te$ opens up a band gap and increases the p-type carrier concentration, which suppresses the bipolar conduction and pushes the Seebeck maximum to a much higher temperature. All the Na-doped samples exhibit lower Seebeck coefficients than the undoped $Pb_{0.6}Sn_{0.4}Te$, which is due to increase in p-type carrier concentration at 300 K.

At 300 K, the Seebeck value increases from $\approx 27.6\ \mu V\,K^{-1}$ to $\approx 48.5\ \mu V\,K^{-1}$ with increasing concentrations of Na from 1 mol% to 4 mol%, respectively (Figure 3c). Interestingly, this trend is reversed at high temperatures. At high temperatures, the Seebeck value decreases with increasing Na concentration from 1 mol% to 4 mol%, and it passes a crossover point at ≈ 430 K (Figure 3c). This can be explained by the two valence band model (light-hole and heavy-hole valence band) of $Pb_{0.6}Sn_{0.4}Te$ (Figure S2).[13,14] The energy difference between these two valence band maxima changes with increasing temperature. At about 450 K, the edges of the two valence bands are at approximately the same energy level, and above 450 K the main contribution to the transport comes from the heavy hole valence band.[13] At 300 K, the increase in Na doping pushes the Fermi level further down into light hole valence band and accesses the heavy hole valence band at high concentrations of Na (Figure S2), which gives rise to high Seebeck values for the 4 mol% Na-doped sample compared to the 1 mol% Na-doped sample. The Seebeck coefficient is directly proportional to density of states effective mass (m^*).[11,12] In PbTe, the heavy hole valence band exhibits higher m^* (1.2–$2\,m_o$) compared to the light hole valence band ($0.2\,m_o$).[12] The crossover point at ≈ 430 K in S versus T data denotes the crossover of light to heavy hole valence band, and above 430 K electrical transport in Na-doped $Pb_{0.6}Sn_{0.4}Te$ is mainly contributed by the heavy hole valence band (Figure S2). At high temperature above 430 K, only the heavy hole band contributes to the electronic transport for 1 mol% Na-doped sample, whereas both light and heavy hole bands contribute in the 4 mol% Na-doped sample because of the lowered Fermi energy (Figure S2). Thus, the Seebeck coefficient of 4 mol% Na-doped sample is lower compared to 1 mol% Na-doped $Pb_{0.6}Sn_{0.4}Te$ at high temperature.

Figure 3d presents the power factor (σS^2) of $Pb_{0.6-x}Sn_{0.4}Na_xTe$ ($x = 0$–0.04) samples as a function of temperature. We obtained the highest power factor of $\approx 21\ \mu W\,cm^{-1}\,K^{-2}$ for 2 mol% Na-doped $Pb_{0.6}Sn_{0.4}Te$ sample at ≈ 856 K, which is significantly higher compared to that of undoped $Pb_{0.6}Sn_{0.4}Te$, owing to increases in both Seebeck coefficient (suppression of bipolar conduction) and electrical conductivity at higher temperatures.

Figure 4a presents the temperature-dependent total thermal conductivity (κ_{total}) of $Pb_{0.6-x}Sn_{0.4}Na_xTe$ ($x = 0$–0.04) samples. κ_{total} of undoped $Pb_{0.6}Sn_{0.4}Te$ shows significant contributions from bipolar thermal conductivity (κ_{bi}) above 450 K, which is suppressed by Na doping owing to the increase in band gap and carrier concentration (Figure 4a). We have quantified the contribution of κ_{bi} at higher temperature (Figure S3). The room temperature κ_{total} value measured for $Pb_{0.58}Sn_{0.40}Na_{0.02}Te$ is $\approx 3.10\ W\,m^{-1}\,K^{-1}$, which decreases to $\approx 1.83\ W\,m^{-1}\,K^{-1}$ at ≈ 873 K. Temperature-dependent lattice thermal conductivity, κ_{latt}, values were obtained by subtracting the electronic thermal conductivity, κ_{el}, from the κ_{total}. The κ_{el} were estimated using the Wiedemann–Franz law, $\kappa_{el} = L\sigma T$; where L is Lorenz number, σ is electrical conductivity, and T is temperature. Temperature-dependent L values were extracted based on the fitting of the respective temperature-dependent S values (Figure S4a) that

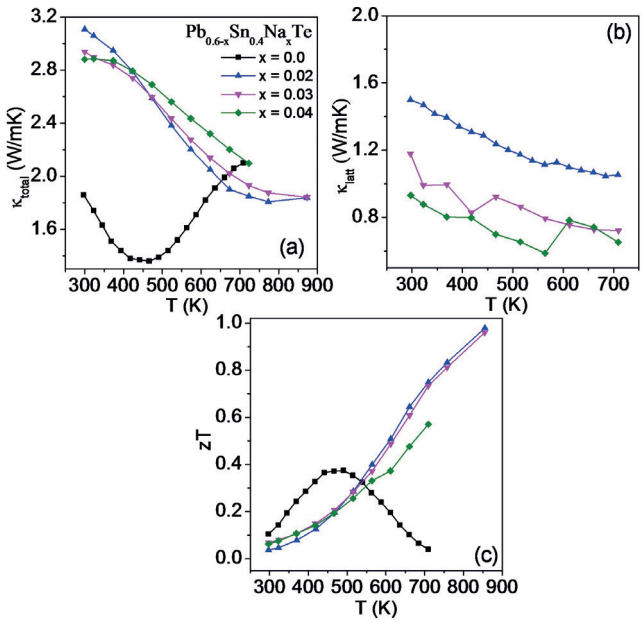

Figure 4. Temperature-dependent a) total thermal conductivity (κ_{total}), b) lattice thermal conductivity (κ_{latt}), and c) thermoelectric figure of merit (zT) of $Pb_{0.6-x}Sn_{0.4}Na_xTe$ ($x = 0$–0.04) samples.

estimate the reduced chemical potential, which was elaborated elsewhere.[4g] The κ_{el} of all the samples are presented in Figure S4b. With increasing Na concentration from 2 to 4 mol%, κ_{latt} value decreases from $\approx 1.5\ W m^{-1} K^{-1}$ to $\approx 0.9\ W m^{-1} K^{-1}$ at 300 K (Figure 4b). It has been shown that Na doping in PbTe introduces point defects and nanoscale precipitates, which collectively reduce the κ_{latt}.[12]

The temperature-dependence of zT of $Pb_{0.6-x}Sn_{0.4}Na_xTe$ ($x = 0$–0.04) samples is shown in Figure 4c. The highest zT value of ≈ 1 at 856 K was achieved for $Pb_{0.58}Sn_{0.40}Na_{0.02}Te$, which is significantly higher compared to undoped $Pb_{0.6}Sn_{0.4}Te$.

In conclusion, Na doping in TCI, $Pb_{0.6}Sn_{0.4}Te$, breaks the local crystal mirror symmetry, which results in modification of the electronic structure and opening of an electronic band gap. Although previous attempts to break the mirror symmetry of TCIs were achieved mainly by physical perturbation techniques, the present work demonstrates that chemistry has a major role in tuning the electronic structure and thermoelectric properties of TCIs. Na doping pushes the Fermi level deeper inside the valence band, which accesses the heavy hole valence band, resulting in improvements in the Seebeck coefficient. Na doping in $Pb_{0.6}Sn_{0.4}Te$ increases p-type carrier concentration and suppresses the bipolar conduction (by opening up a band gap), which collectively improve the thermoelectric properties. These results should motivate chemists to explore various doping strategies that may modify/tune the electronic structure and properties of TCIs.

Acknowledgements

This work was supported by Ramanujan Fellowship (SERB) and Sheikh Saqr Laboratory. S.R. thanks CSIR for fellowship. U.V.W. acknowledges funding from JC Bose National Fellowship, DST, India. We thank Arpan Dey for his help during Hall measurements. We thank Prof. C. N. R. Rao for constant support.

Keywords: chemical doping · crystal symmetry breaking · electronic structures · thermoelectrics · topological crystalline insulator

How to cite: *Angew. Chem. Int. Ed.* **2015**, *54*, 15241–15245
Angew. Chem. **2015**, *127*, 15456–15460

[1] a) L. Müchler, H. Zhang, S. Chadov, B. Yan, F. Casper, J. Kübler, S. C. Zhang, C. Felser, *Angew. Chem. Int. Ed.* **2012**, *51*, 7221; *Angew. Chem.* **2012**, *124*, 7333; b) D. Hsieh, D. Qian, L. Wray, Y. Xia, Y. S. Hor, R. J. Cava, M. Z. Hasan, *Nature* **2008**, *452*, 970; c) X. L. Qi, S. C. Zhang, *Phys. Today* **2010**, *63*, 33; d) M. Z. Hasan, C. L. Kane, *Rev. Mod. Phys.* **2010**, *82*, 3045; e) J. Moore, *Nature* **2010**, *464*, 194; f) X. L. Qi, S. C. Zhang, *Rev. Mod. Phys.* **2011**, *83*, 1057; g) B. Yan, S. Zhang, *Rep. Prog. Phys.* **2012**, *75*, 096501.

[2] a) G. Xiao, C. Zhu, Y. Ma, B. Liu, G. Zou, B. Zou, *Angew. Chem. Int. Ed.* **2014**, *53*, 729; *Angew. Chem.* **2014**, *126*, 748; b) Z. H. Wang, L. Yang, X. J. Li, X. T. Zhao, H. L. Wang, Z. D. Zhang, X. P. A. Gao, *Nano Lett.* **2014**, *14*, 6510; c) A. Chatterjee, K. Biswas, *Angew. Chem. Int. Ed.* **2015**, *54*, 5623; *Angew. Chem.* **2015**, *127*, 5715.

[3] a) D. Kong, Y. Cui, *Nat. Chem.* **2011**, *3*, 845; b) X. Wang, Y. Du, S. Dou, C. Zhang, *Phys. Rev. Lett.* **2012**, *108*, 266806.

[4] a) L. Müchler, F. Casper, B. Yan, S. Chadovand, C. Felser, *Phys. Status Solidi RRL* **2013**, *7*, 91; b) J. Sootsman, D. Y. Chung, M. G. Kanatzidis, *Angew. Chem. Int. Ed.* **2009**, *48*, 8616; *Angew. Chem.* **2009**, *121*, 8768; c) L. D. Zhao, V. P. Dravid, M. G. Kanatzidis, *Energy Environ. Sci.* **2014**, *7*, 251; d) G. J. Snyder, E. S. Toberer, *Nat. Mater.* **2008**, *7*, 105; e) K. Biswas, J. He, Q. Zhang, G. Wang, C. Uher, V. P. Dravid, M. G. Kanatzidis, *Nat. Chem.* **2011**, *3*, 160; f) K. Biswas, J. He, I. D. Blum, C. I. Wu, T. P. Hogan, D. N. Seidman, V. P. Dravid, M. G. Kanatzidis, *Nature* **2012**, *489*, 414; g) S. N. Guin, A. Chatterjee, D. S. Negi, R. Datta, K. Biswas, *Energy Environ. Sci.* **2013**, *6*, 2603.

[5] a) T. Sato, Y. Tanaka, K. Nakayama, S. Souma, T. Takahashi, S. Sasaki, Z. Ren, A. A. Taskin, K. Segawa, Y. Ando, *Phys. Rev. Lett.* **2013**, *110*, 206804; b) Y. Ando, L. Fu, *Annu. Rev. Condens. Matter Phys.* **2015**, *6*, 361; c) L. Fu, *Phys. Rev. Lett.* **2011**, *106*, 106802; d) J. Liu, T. H. Hsieh, P. Wei, W. Duan, J. Moodera, L. Fu, *Nat. Mater.* **2014**, *13*, 178; e) I. Zeljkovic, Y. Okada, M. Serbyn, R. Sankar, D. Walkup, W. Zhou, J. Liu, G. Chang, Y. J. Wang, M. Z. Hasan, F. Chou, H. Lin, A. Bansil, L. Fu, V. Madhavan, *Nat. Mater.* **2015**, *14*, 318; f) T. Liang, Q. Gibson, J. Xiong, M. Hirchberger, S. P. Koduvayur, R. J. Cava, N. P. Ong, *Nat. Commun.* **2013**, *4*, 2696; g) K. V. Mitrofanov, A. V. Kolobov, P. Fons, M. Krbal, J. Tominaga, T. Uruga, *J. Phys. Condens. Matter* **2014**, *26*, 475502; h) I. Zeljkovic, Y. Okada, C.-Y. Huang, R. Sankar, D. Walkup, W. Zhou, M. Serbyn, F. Chou, W.-F. Tsai, H. Lin, A. Bansil, L. Fu, M. Z. Hasan, V. Madhavan, *Nat. Phys.* **2014**, *10*, 572; i) Y. Okada, M. Serbyn, H. Lin, D. Walkup, W. Zhou, C. Dhital, M. Neupane, S. Xu, Y. J. Wang, R. Sankar, F. Chou, A. Bansil, M. Z. Hasan, S. D. Wilson, L. Fu, V. Madhavan, *Science* **2013**, *341*, 1496; j) A. S. Erickson, J. H. Chu, M. F. Toney, T. H. Geballe, I. R. Fisher, *Phys. Rev. B* **2009**, *79*, 024520.

[6] a) T. H. Hsieh, H. Lin, J. Liu, W. Duan, A. Bansil, L. Fu, *Nat. Commun.* **2012**, *3*, 982; b) Y. Tanaka, T. Sato, K. Nakayama, S. Souma, T. Takahashi, Z. Ren, M. Novak, K. Segawa, Y. Ando, *Phys. Rev. B* **2013**, *87*, 155105; c) M. Serbyn, L. Fu, *Phys. Rev. B* **2014**, *90*, 035402; d) E. Tang, L. Fu, *Nat. Phys.* **2014**, *10*, 964;

e) X. Qian, L. Fu, J. Li, *Nano Res.* **2015**, *8*, 967; f) L. Fu, C. L. Kane, *Phys. Rev. Lett.* **2012**, *109*, 246605.
[7] U. Kattner, H. L. Lukas, G. Petzow, B. Gather, E. Irle, R. Blachnik, *Z. Metallkd.* **1988**, *79*, 32.
[8] a) Q. Zhang, B. Liao, Y. Lan, K. Lukas, W. Liu, K. Esfarjani, C. Opeil, D. Broido, G. Chen, Z. Ren, *Proc. Natl. Acad. Sci. USA* **2013**, *110*, 13261; b) G. Tan, F. Shi, J. W. Doak, H. Sun, L. D. Zhao, P. Wang, C. Uher, C. Wolverton, V. P. Dravid, M. G. Kanatzidis, *Energy Environ. Sci.* **2015**, *8*, 267; c) A. Banik, U. S. Shenoy, S. Anand, U. V. Waghmare, K. Biswas, *Chem. Mater.* **2015**, *27*, 581; d) A. Banik, K. Biswas, *J. Mater. Chem. A* **2014**, *2*, 9620.
[9] S. Y. Xu, C. Liu, N. Alidoust, M. Neupane, D. Qian, I. Belopolski, J. D. Denlinger, Y. J. Wang, H. Lin, L. A. Wray, G. Landolt, B. Slomski, J. H. Dil, A. Marcinkova, E. Morosan, Q. Gibson, R. Sankar, F. C. Chou, R. J. Cava, A. Bansil, M. Z. Hasan, *Nat. Commun.* **2012**, *3*, 1192.
[10] a) J. O. Dimmock, I. Melngailis, A. J. Strauss, *Phys. Rev. Lett.* **1966**, *16*, 1193; b) X. Gao, M. S. Daw, *Phys. Rev. B* **2008**, *77*, 033103.
[11] Y. Pei, A. LaLonde, S. Iwanaga, G. J. Snyder, *Energy Environ. Sci.* **2011**, *4*, 2085.
[12] a) J. Androulakis, I. Todorov, D.-Y. Chung, S. Ballikaya, G. Wang, C. Uher, M. Kanatzidis, *Phys. Rev. B* **2010**, *82*, 115209; b) J. He, L.-D. Zhao, J.-C. Zheng, J. W. Doak, H. Wu, H.-Q. Wang, Y. Lee, C. Wolverton, M. G. Kanatzidis, V. P. Dravid, *J. Am. Chem. Soc.* **2013**, *135*, 4624.
[13] a) R. S. Allgaier, *J. Appl. Phys.* **1961**, *32*, 2185; b) R. S. Allgaier, B. B. Houston, *J. Appl. Phys.* **1966**, *37*, 302; c) S. V. Airapetyants, M. N. Vinogradova, I. N. Dubrovskaya, N. V. Kolomoets, I. M. Rudnik, *Sov. Phys. Solid State* **1966**, *8*, 1069.
[14] Y. Pei, X. Shi, A. LaLonde, H. Wang, L. Chen, G. J. Snyder, *Nature* **2011**, *473*, 66.

Received: September 10, 2015
Revised: October 8, 2015
Published online: October 28, 2015

